Journal of Alloys and Compounds 320 (2001) 242–250

Journal of ALLOYS AND COMPOUNDS

www.elsevier.com/locate/jallcom

# Heat capacity and phase equilibria in rare earth alloy systems. R-rich R-Al alloys (R=La, Pr and Nd)

G. Borzone[a], N. Parodi[a], R. Ferro[a,]*, J.P. Bros[b], J.P. Dubès[c], M. Gambino[b]

[a]*Dipartimento di Chimica e Chimica Industriale, Sezione di Chimica Inorganica e Metallurgia, Via Dodecaneso 31, Università di Genova, I-16146 Genova, Italy*
[b]*Université de Provence, IUSTI-CNRS, 5, rue Enrico Fermi, 13453 Marseille, Cedex 13, France*
[c]*Laboratoire de Thermochimie, Université de Provence, Centre de St. Charles, 3 place V. Hugo, 13331 Marseille, Cedex 3, France*

**Abstract**

Molar heat capacities of the R-Al (R=La, Pr and Nd) R-rich alloys were determined at different temperatures by differential scanning calorimetry both by using the stepwise and the enthalpimetric methods. The results obtained for the molar heat capacity of $\alpha Pr_3Al$, $\beta Pr_3Al$ and $Nd_3Al$ phases have been reported together with the values obtained for liquid La–Al alloys ($x_{Al}=0.25$). The characteristic temperatures obtained for the different invariant reaction involved in the R-rich region have been compared with the literature data. The $\alpha \leftrightarrow \beta Pr_3Al$ transformation has been confirmed at 330°C and a value of $\Delta_{trs}H \cong +0.09$ kJ/mol of atoms obtained for the transformation enthalpy. © 2001 Elsevier Science B.V. All rights reserved.

*Keywords:* Molar heat capacity; Rare earth-aluminum alloys; Thermodynamic properties; Calorimetry

## 1. Introduction

The recent development of differential scanning calorimeters (DSC) makes it possible to obtain reliable molar heat capacity ($C^{o}_{p,m}$) data on large temperature ranges, even though, until now, with this technique $C^{o}_{p,m}=f(T)$ measurements at very low temperature ($T<-100$°C) are not possible. DSC measurements are interesting for practical purposes. As already shown [1,2], moreover, precise determination of the molar heat capacity versus temperature and as a function of the composition of a material can give information for a better knowledge of the equilibrium phase diagrams and their thermodynamic optimization, which would make the extrapolation from binary to complex systems possible in many cases.

Among the materials that we are interested in, several rare earth alloy systems may be considered. In particular, rare earths (R) are important alloying elements to aluminium alloys because of their ability to enhance the high temperature properties and casting characteristics. Besides, rapidly solidified Al-R metal alloys also offer the possibility of obtaining better corrosion behaviour [3,4].

The importance of a detailed knowledge of the complete phase diagrams involved, not only in the Al-rich portions, as well as of the thermodynamic properties is then obvious.

In this paper we present the experimental results obtained on the molar heat capacity of Al–La, Al–Pr and Al–Nd alloys and information on the constitutional properties of the R-rich alloys.

## 2. Literature data

### 2.1. The La–Al system

Fig. 1a shows the phase diagram assessed by Gschneidner [5] mainly on the basis of the investigation of Buschow [6]. The La-rich side has been adjusted according to the recent work performed by Saccone et al. [7]. A temperature of 530°C instead of 547°C, and a composition of 23.0 at.%Al were proposed for the eutectic reaction L↔βLa+LaAl instead of the reaction $L \leftrightarrow \beta La + La_3Al$. Moreover, the $La_3Al$ was found to form by peritectoid reaction at about 520°C and to decompose into βLa and LaAl at a temperature slightly higher than 400°C. The Al-rich portion has recently been studied by Kononenko and Golubev [8]. A temperature of 636°C (instead of

---

*Corresponding author. Tel.: +39-010-353-6149/6161; fax: +39-010-362-5051.

*E-mail address:* ferro@chimica.unige.it (R. Ferro).

0925-8388/01/$ – see front matter
PII: S0925-8388(00)01471-7

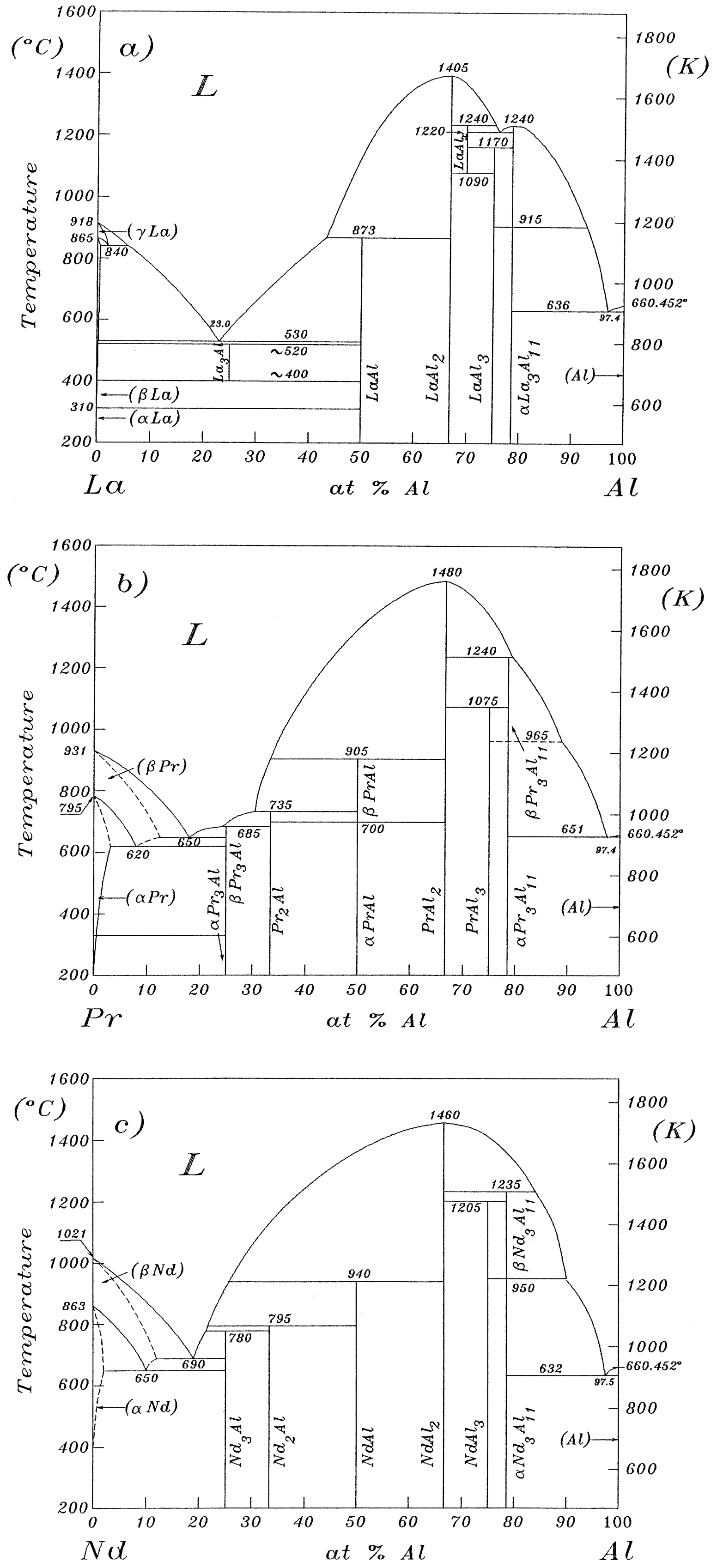

Fig. 1. Al systems with La, Pr, Nd. Phase diagrams according to the literature data (temperature values in °C): La–Al [5–8]; Pr–Al [7,8,12], Nd–Al [7,8,19,20].

640°C) and $x_{\mathrm{Al}}=0.974$ has been suggested for the eutectic reaction.

The literature data relevant to the La–Al phases concerning our investigation are reported in Table 1, together with the results of this work.

### 2.2. The Pr–Al system

The assessed version of the phase diagram proposed by Gschneidner and Calderwood [12] is based on the investigations by Buschow et al. [13–15] and by Drits et al. [16]. Considering the more recent studies reported by Saccone et al. [7] and Kononenko and Golubev [8], the modified version given in Fig. 1b differs in several respects from that proposed by Gschneidner and Calderwood [12].

The following variations have been inserted: the eutectoid reaction βPr↔αPr+β$\mathrm{Pr_3Al}$ occurring at 620°C (instead of the previous reported reaction at 630°C corresponding to the peritectoid formation of β$\mathrm{Pr_3Al}$ from αPr and $\mathrm{Pr_2Al}$), the eutectic reaction L↔βPr+β$\mathrm{Pr_3Al}$ occurring at 650°C and 17.5 at.%Al (in good agreement with the values reported by Buschow) and the peritectic reaction L+$\mathrm{Pr_2Al}$↔β$\mathrm{Pr_3Al}$ at 685°C.

$\mathrm{Pr_3Al}$ was found to exist in two stuctures: α$\mathrm{Pr_3Al}$ (*hP8*-$\mathrm{Ni_3Sn}$ type) stable at low temperature (below about 330°C) and the β$\mathrm{Pr_3Al}$ form, *cP4*-$\mathrm{AuCu_3}$ type, stable at high temperature. For the Al-rich eutectic reaction, the temperature of 640°C and the composition ($x_{\mathrm{Al}}\approx0.95$) reported by Buschow and van Vucht [13] were modified into 651°C and $x_{\mathrm{Al}}=0.976$, respectively, according to the measurements performed by Mondolfo [17] and Kononenko [8] and the assessment by Okamoto [18].

The literature data relevant to the Pr–Al phases together with the results now obtained are summarized in Table 1.

### 2.3. The Nd–Al system

The phase diagram of the Nd–Al system was determined by Buschow [19] and assessed by Gschneidner and Calderwood [20]. Fig. 1c shows the modified version, on the basis of the recent investigations performed in the Nd-rich [7] and Al-rich regions [8]. The following varia-

Table 1
La–Al, Pr–Al and Nd–Al systems (thermal data relevant to the R-rich alloys)

| Transition | T (°C) | Remarks | Ref. |
|---|---|---|---|
| Al(1)↔Al(Cr) | 660.452 | | [9] |
| La(l)↔γLa | 918 | | [10] |
| γLa↔βLa | 865 | | [10] |
| βLa ↔ αLa | 260 | on cooling | [10] |
| | 310 | on heating | [10] |
| | 277±40 | | [11] |
| βLa+LaAl↔$\mathrm{La_3Al}$ | ~520 | DTA on cooling, 10°C/min | [7] |
| | 520–525 | stepwise $C_p$ measurements every 5°C, on heating, (Fig. 2b) | t.w. |
| | 530–535 | enthalpimetric analysis, 2°C/min on heating, (Fig. 3) | t.w. |
| $\mathrm{La_3Al}$↔βLa+LaA1 | ~400 | estimated by quenching experiments | [7] |
| | 430–440 | stepwise $C_p$ measurements, every 5°C on heating | t.w. |
| | 350–450° | stepwise $C_p$ measurements, every 10°C on heating, (see Fig. 2a) | t.w. |
| | 440 | enthalpimetric analysis 2°C/min, on heating | t.w. |
| L(23.3 at.%Al)↔βLa+$\mathrm{La_3Al}$ | 547 | replaced by the following eutectic reaction (LaAl instead of $\mathrm{La_3Al}$) | [5,6] |
| L(23.0 at.%Al)↔βLa+LaAl | 530 | | [7] |
| | 540–545 | stepwise $C_p$ measurements, every 5°C on heating, (see Fig. 2b) | t.w. |
| | 545 | enthalpimetric analysis 2°C/min, on heating, (see Fig. 3) | t.w. |
| Pr(l)↔βPr | 931 | | [10] |
| βPr↔αPr | 795 | | [10] |
| L+$\mathrm{Pr_2Al}$↔β$\mathrm{Pr_3Al}$ | 685 | | [7] |
| | 680–685 | stepwise $C_p$ measurements, every 5°C on heating, (see text) | t.w. |
| L(≈18 at.%Al)↔αPr+$\mathrm{Pr_2Al}$ | 650 | reaction not confirmed, see the following eutectic | [13] |
| L(17.5 at.%Al)↔βPr+β$\mathrm{Pr_3Al}$ | 650 | | [7] |
| | 645 | stepwise $C_p$ measurements; every 5°C on heating, (Fig. 4b) | t.w. |
| (αPr+$\mathrm{Pr_2Al}$↔β$\mathrm{Pr_3Al}$) | 630 | reaction not confirmed | [13] |
| βPr(8.0 at.%Al)↔αPr+β$\mathrm{Pr_3Al}$ | 620 | | [7] |
| | 625–630 | stepwise $C_p$ measurements, every 5°C on heating, (Fig. 4b) | t.w. |
| β$\mathrm{Pr_3Al}$↔α$\mathrm{Pr_3Al}$ | ~330 | | [12,13] |
| | 330 | stepwise $C_p$ measurements, every 10°C on heating, (Fig. 4a) | t.w. |
| Nd(1)↔βNd | 1021 | | [10] |
| βNd↔αNd | 863 | | [10] |
| βNd (10.0 at.%Al)↔αNd+$\mathrm{Nd_3Al}$ | 650 | | [7] |
| | 650 | stepwise $C_p$ measurements, every 5°C on heating, (see text) | t.w. |
| L(≈15 at.%Al)↔αNd+$\mathrm{Nd_3Al}$ | 635 | replaced by the following eutectic reaction (βNd instead of αNd) | [19] |
| L(19.0 at.%Al)↔βNd+$\mathrm{Nd_3Al}$ | 690 | | [7] |
| | 685 | stepwise $C_p$ measurements, every 5°C on heating | t.w. |

tions have been reported: the eutectoid reaction $\beta Nd \leftrightarrow \alpha Nd + Nd_3Al$ occurring at 650°C and 10.0 at.%Al and the eutectic reaction $L \leftrightarrow \beta Nd + Nd_3Al$ occurring at 690°C and 19.0 at.%Al. In the previous version, only the existence of the eutectic reaction was proposed, at 15.0 at.%Al and a temperature of 635°C. The peritectic temperature of 795°C for the formation of $Nd_2Al$ has been inserted according to Buschow [19].

Following the investigation carried out by Kononenko [8] and the assessment by Okamoto [21], the temperature of 632°C (instead of 640°C) and $x_{Al}=0.975$ for the $L \leftrightarrow \alpha Nd_3Al_{11} + (Al)$ eutectic reaction have also been inserted in the Al-rich side.

The literature data relevant to the Nd–Al phases and those concerning our investigation are reported in Table 1.

### 2.4. Thermodynamic properties

A number of thermodynamic investigations of the liquid and solid alloys of Al with the light R, are reported in literature. A summary of the data concerning the enthalpy of formation of the solid alloys relevant to this investigation are given in Table 2 together with the heat capacity, standard entropy and heats of transformation and fusion of the metals involved.

Different techniques, e.m.f., acid solution [25,26] and aluminium solution calorimetry [27,28], direct drop calorimetry [29,30] and direct reaction calorimetry [22–24] have been used. Three different calorimeters were used for the determination of the partial and integral enthalpy of mixing [28]. The enthalpy of mixing of liquid aluminium–lanthanum alloys was measured calorimetrically at 1650°C [31] and the Gibbs free energy, enthalpy and entropy of alloying were determined from vapour pressure measurements at 1150–1420°C over the whole concentration range [32].

E.m.f. measurements at 670–870 K were used by Kober et al. [33] to study the formation of Nd–Al intermetallic compounds and the corresponding thermodynamic properties. The Knudsen effusion method to investigate the vapour pressure of Al over the Nd–Al alloys at 1700 K has been used by Shevchenko et al. [34] and the activities of molten alloys have been obtained. The enthalpy of mixing of Pr–Al and Nd–Al liquid systems were investigated by high temperature calorimetry at 1250–1550 K [35], and temperature-concentration dependence has been studied.

## 3. Experimental

### 3.1. Preparation of the samples

Starting materials were lanthanum, praseodymium and neodymium with nominal purities of 99.9 mass% and aluminium 99.999 mass%, respectively. Samples were prepared with the following compositions: La–Al $x_{Al}=$ 0.23, 0.25 and 0.26; Pr–Al $x_{Al}=0.24$, 0.25 and 0.26; and Nd–Al $x_{Al}=0.24$. Preparation was performed by weighing stoichiometric amounts of the two metals (about 700 mg), enclosed in tantalum gas-tight cylindrical crucibles (∅=6 mm, height 12 mm), sealed by arc-welding under argon. This allowed us to avoid any mass-loss, variation in the composition and oxidation of the samples. The samples were induction-heated in an argon atmosphere. Annealing and quenching were then carried out in order to obtain the alloys in well-defined conditions.

### 3.2. Heat capacity measurements

The alloys were examined by means of a differential scanning calorimeter. The apparatus used is designed as a Calvet calorimeter, where two cylindrical cells (reference and working cells) are surrounded by two differentially connected thermal fluxmeters (thermopiles). This kind of

Table 2
Thermodynamic properties for La, Pr, Nd elements and La–Al, Pr–Al and Nd–Al, R-rich alloys

| Phase | Ref. | Heat capacity at 298 K $C^o_{p,m}$ (J/mol at.K) | Standard entropy $S^o_{298}$ (J/mol at.K) | Transformation enthalpy $\Delta_{trs}H$ (kJ/mol at.) | Melting enthalpy $\Delta_{fus}H^o$ (kJ/mol at.) | Formation enthalpy $\Delta_f H^o$ (kJ/mol at.) |
|---|---|---|---|---|---|---|
| Al | [11] | 24.3 | 28.3 | | 10.7 | |
| La | [10,11] | 27.1 | 56.9 | $\alpha La \leftrightarrow \beta La$ 0.36 | 6.20 | |
| | [10,11] | | | $\beta La \leftrightarrow \gamma La$ 3.12 | | |
| LaAl | [22] | | | | | $-46.0\pm2$ |
| Pr | [10,11] | 27.4 | 73.9 | $\alpha Pr \leftrightarrow \beta Pr$ 3.17 | 6.89 | |
| $\alpha Pr_3Al$ | [23] | | | | | $-25.0\pm2^a$ |
| | t.w. | 23.9 | | $\alpha Pr_3Al \leftrightarrow \beta Pr_3Al$ $0.09^b$ | | |
| $\beta Pr_3Al$ | t.w. | $(21.9^c)$ | | | | |
| Nd | [10,11] | 27.4 | 71.1 | $\alpha Nd \leftrightarrow \beta Nd$ 3.03 | 7.14 | |
| | | | | | | $-27.5\pm2$ |
| $Nd_3Al$ | [24] | | | | | |
| | t.w. | 22.3 | | | | |

[a] Interpolated value from the enthalpy/composition curve.

[b] Estimated from $C_p$ measurements in the $330<T/°C<380$ temperature range.

[c] Extrapolated value for the $\beta Pr_3Al$ phase, metastable at $T<330°C$ (603 K).

Table 3
Heat capacity of selected R-Al alloys

| Alloy system | $x_{Al}$ | Phase | $C^o_{p,m}=a+b\times10^{-3}\ (T-T_0)$ $T_0=298.15$ K (J $K^{-1}$ mol at. $^{-1}$) | | Temperature range | |
|---|---|---|---|---|---|---|
| | | | $a$ | $b$ | (K) | (°C) |
| La–Al | 0.25 | Liquid, (Fig. 2b) | 51.1 | −25.7 | 868–923 | 595–650 |
| | 0.26 | Liquid | 52.8 | −22.7 | 883–923 | 610–650 |
| Pr–Al | 0.25 | $\alpha Pr_3Al$ | 23.9 | 17.1 | 423–593 | 150–320 |
| | 0.25 | $\beta Pr_3Al$ | 21.9 | 31.2 | 613–833 | 340–560 |
| Nd–Al | 0.24 | $Nd_3Al$ | 22.3 | 20.5 | 323–833 | 50–560 |

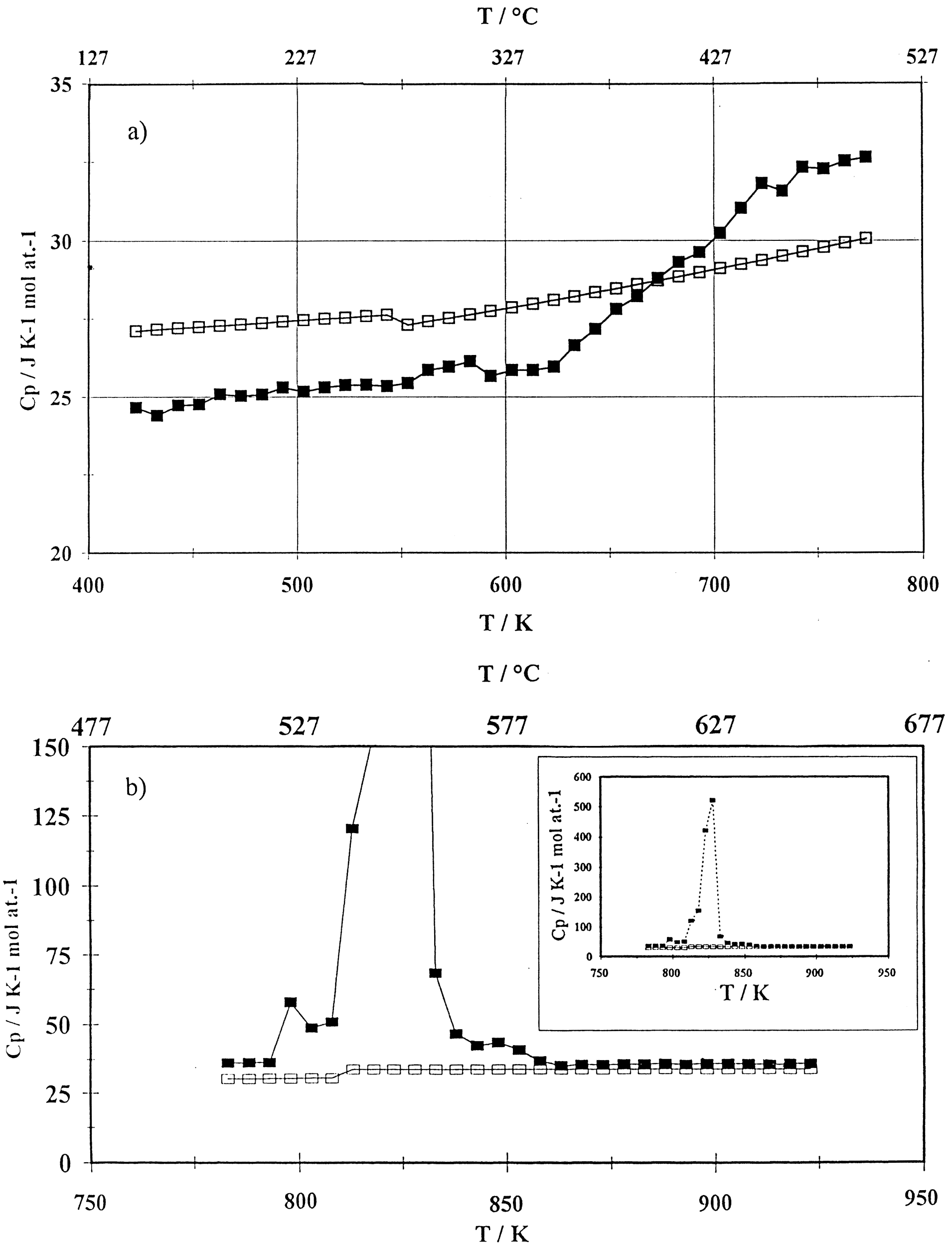

Fig. 2. La–Al system. Experimental molar heat capacity of La–Al ($x_{Al}=0.25$) alloy vs. temperature: □, calculated values obtained from the Neumann–Kopp rule; (a) ■, experimental values measured step by step every 10°C ($150<T/°C<500$); (b) ■, experimental values every 5°C ($510<T/°C<650$).

apparatus can be used in two different ways, either heating step by step to measure $C^{o}_{p,m}$ or by continuous heating to perform enthalpimetric analysis.

According to the first method, from the observation of the thermal disequilibrium between the two cells during a heat pulse, the heat capacity of the sample located in the working cell can be obtained as a function of the temperature. The two tantalum crucibles contained in the cells are chosen in order to have as similar a mass as possible. During the experiment, the cells are maintained in a purified argon flow. In the temperature range from 50 to 700°C, the $C^{o}_{p,m}$ measurements are carried out step by step every 5 or 10°C by heating for 200 s, and maintaining a constant temperature plateau for 400 s. The details of the experimental procedure have been described elsewhere [2,36].

Before each experiment, the calorimeter was calibrated. Two calibration methods were employed: generally a standard NIST (National Institute of Standards and Technology) α alumina crystal was used for comparison. Periodically, direct Joule heating of an electrical resistance located in the cell was used. Temperatures were measured at 0.5°C and molar heat capacity with an accuracy of about 2%.

By using the same equipment in continuous heating mode at a rate from 2 to 5°C/min, the temperature and heat of transformation have been determined. In this case the calibration of the apparatus was performed with measurements of the temperature and heat of melting of pure metallic In, Sn, Pb and Zn elements. The melting points were determined to be within ±0.5 K of the Barin values [11].

To accumulate the complete set of data for the present investigation, generally a series of different runs in various temperature ranges were made and, in order to verify consistency, each run was repeated three times or more.

## 4. Results

In all cases the quantity $[xC^{o}_{p,m}(\mathrm{Al})+(1-x)C^{o}_{p,m}(\mathrm{R})]$ was evaluated and used in order to define a reference slope for the heat capacity data. For the pure elements, the heat capacity values reported in the Barin compilation [11] were used. The characteristic transformation temperatures accepted for the pure elements are reported in Table 1.

The experimental values of $C^{o}_{p,m}$ vs. $T$ (K) for the different compounds have been represented by the following equation:

$$C^{o}_{p,m} = a + b \times 10^{-3}\,(T - T_0)\ (\mathrm{J/K\ mol.\ at.})$$

with $T_0 = 298.15$ K, where the $a$ and $b$ values were obtained by a least-squares fitting.

### 4.1. Al–La system

We have investigated three alloys having $x_{\mathrm{Al}} = 0.23$, 0.25, 0.26 molar fractions, held, after melting, for equilibration for 1 week at 220°C. The molar heat capacity of these alloys has been measured step by step every 10°C in the $50 < T/°\mathrm{C} < 350$, $150 < T/°\mathrm{C} < 560$ and every 5°C in the $510 < T/°\mathrm{C} < 650$ temperature ranges, respectively. A part of the experimental data (molar heat capacity) are given in Table 3 and Fig. 2.

No α↔β transformation is presented by $La_3Al$, unlike $Pr_3Al$. $La_3Al$ has the *hP8*-$Ni_3Sn$ type structure; it is however stable only as a high temperature phase (see Fig. 1a).

The values observed for the different invariant reactions are compared in Table 1. A good agreement with the literature data may generally be noticed.

A sluggishness was observed for the formation in the solid state on heating of $La_3Al$ according to the reaction $\beta La + LaAl \leftrightarrow La_3Al$. Starting from heat capacity measurements performed every 10°C, the effect is broadest between 350° and 450°C (see Table 1 and Fig. 2a). In the stepwise heat capacity measurements performed on $x_{\mathrm{Al}} =$ 0.23, 0.25 and 0.26 alloys by increasing temperature by step of 5°C, this transformation is recorded at 430–440°C (see Table 1). For the sample with $x_{\mathrm{Al}} = 0.25$, between 520° and 525°C, a thermal effect corresponding to the decomposition of $La_3Al$ may be observed (Fig. 2b), followed on heating by the eutectic reaction.

The eutectic reaction $L \leftrightarrow \beta La + LaAl$ was observed at about 540–545°C. The enthalpimetric analysis performed on heating at a scanning rate of 2°C/min in the 300–620°C temperature range on samples having $x_{\mathrm{Al}} = 0.23$ and 0.26 compositions confirm this temperature. The 450–620°C portion of the heating curves is shown in Fig. 3. In similar runs, a slight deviation from the base-line observed at $T \approx 440$°C for the sample having $x_{\mathrm{Al}} = 0.23$, may be related

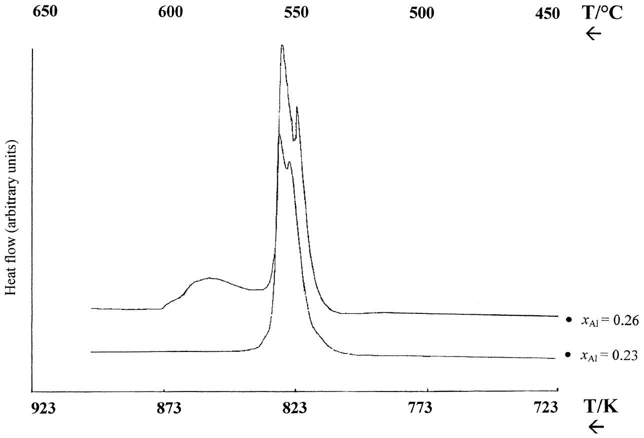

Fig. 3. La–Al alloys ($x_{\mathrm{Al}} = 0.23$, 0.26). Enthalpimetric analysis at heating scanning rate of 2°C/min.

to the above mentioned synthesis of $La_3Al$, in agreement with the results obtained by the stepwise method.

From the same alloys, an indication of the liquidus temperature was also obtained ($T$ about 570°C at $x_{Al}=0.23$; 580°C at $x_{Al}=0.25$ and 605°C at $x_{Al}=0.26$). This seems to suggest an eutectic composition slightly less than 23 at.%Al (22.5 at.%Al ?). Owing to the above-mentioned sluggishness observed for the synthesis of $La_3Al$, and the small temperature range in which this phase exists, it was not possible to calculate an equation $C^{o}_{p,m}=f(T)$.

For the different samples the experimental values of $C^{o}_{p,m}$ for the liquid phase as a function of the temperature are reported in Table 3.

### 4.2. Pr–Al system

Three alloys with $x_{Al}=0.24$, 0.25, 0.26 composition have been studied. These have been annealed for 4 days at 280°C and 4 days at 220°C. The molar heat capacity of $Pr_3Al$ compound has been measured step by step every

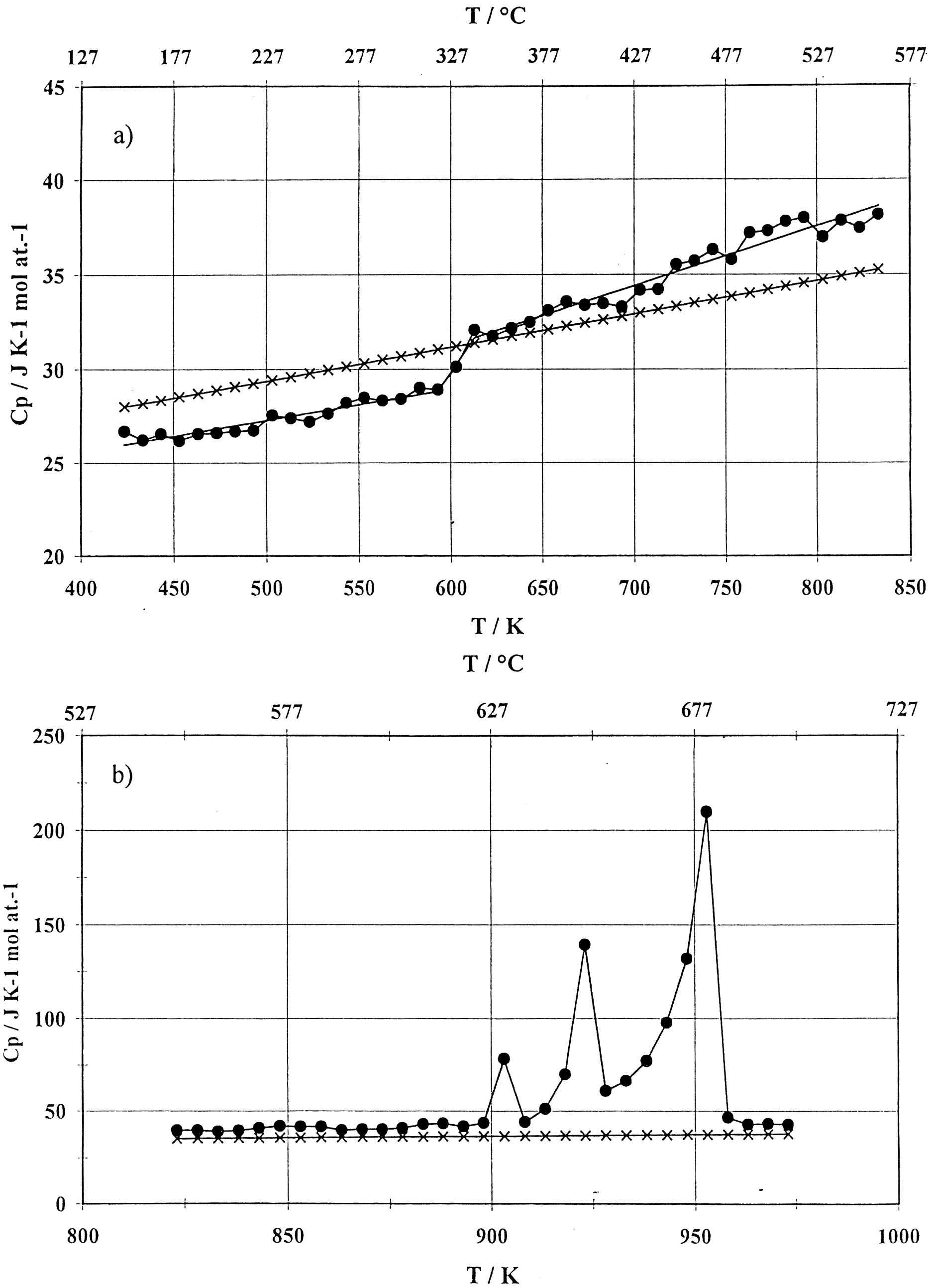

Fig. 4. Pr–Al system. X calculated values obtained from the Neumann–Kopp rule; (a) Pr–Al alloy with $x_{Al}=0.25$: ● experimental molar heat capacity values measured step by step every 10°C ($150<T/°C<560$); (b) Pr–Al alloy with $x_{Al}=0.24$: ● experimental molar heat capacity values every 5°C ($550<T/°C<700$).

10°C in the 50–350°C and 150–560°C temperature range. Investigation every 5°C was performed in the 550–700°C temperature range. Fig. 4a shows an effect at 330°C, which can be related to the $\alpha\leftrightarrow\beta Pr_3Al$ transformation in very good agreement with the previous value (~330°C) reported by Buschow [13,14]. Owing to the small value of the heat associated to this transformation (about 90 J/mol at., see Table 2) this effect was observed only by using the step by step method.

For an alloy with a Pr content slightly less than $Pr_3Al$, $x_{Al}=0.24$, Fig. 4b shows, in agreement with the literature data [7], an effect at 625–630°C (eutectoid equilibrium), another effect at 645°C (Pr-rich eutectic equilibrium), followed by the two-phase liquid + $Pr_3Al$ region ending at 680–685°C.

The results obtained on samples having nominal composition $x_{Al}=0.25$ and 0.26, clearly show the peritectic equilibrium at 680°C followed by a small two-phase region ending at about 690°C. The equations of the molar heat capacity obtained for the $\alpha Pr_3Al$ in the 150–320°C and for the $\beta Pr_3Al$ form in the 340–560°C temperature range are reported in Table 3.

### *4.3. Nd–Al system*

Only one sample was prepared at $x_{Al}=0.24$; after melting it was annealed for 4 days at $T=280$°C and for 4 days at 220°C.

The heat capacity measurements were carried out every 10°C in the temperature range from 50°C to 560°C, every 5°C in the range 550–700°C. No indication of a solid phase transformation was observed in these temperature ranges.

The thermal effects detected at $T=650$°C and $T=685$°C correspond to the eutectoid decomposition of $\beta Nd\leftrightarrow\alpha Nd+Nd_3Al$ and to the eutectic reaction $L\leftrightarrow\beta Nd+Nd_3Al$, respectively, in good agreement with the literature data [7].

For the $Nd_3Al$ compound the interpolated $C^{o}_{p,m}$ value now obtained ($50° < T < 560$°C) is reported in Table 3.

## 5. General remarks

In this case, as observed for other rare earth binary alloys, negative $\Delta_f C^{o}_{p,m}$ (about −3 to −4 J/mol at. K) have been generally observed for $\alpha Pr_3Al$ and $Nd_3Al$. On the other hand, slightly positive $\Delta_f C^{o}_{p,m}$ have been observed for the high temperature phases: $La_3Al$ and $\beta Pr_3Al$.

In conclusion we may note the interest and versatility of the heat capacity measurements in defining selected constitutional properties of alloys for which the equilibria involved cannot be easily determined by using other techniques. This has already been underlined in the investigation performed on other binary systems [1,2]. Paticularly useful can be the coupled employment of the enthalpimetric analysis and the step by step heat capacity measurements. The first one is very reliable in the case of solid–liquid transformation, while, for reactions characterized by small heat effects such as in the solid–solid transformation, the stepwise method is especially favourable.

A quantitative evaluation of the transformation enthalpy, moreover, is very useful for a further assessment of the system, based on a thermodynamic optimization.

## Acknowledgements

This contribution has been prepared in memoriam of Alan Prince, whose scientific work and human qualities are important reference points for all of the authors. We would like to thank the 96 GALILEO Program, for the financial support afforded us. The Italian authors acknowledge with thanks the financial support from the Italian Ministero della Ricerca Scientifica e Tecnologica ‘Programmi di Ricerca Scientifica di Rilevante Interesse Nazionale’ and from the Italian National Research Council (CNR) ‘Progetto Finalizzato Materiali Speciali per Tecnologie Avanzate MSTAII’.

## References

[1] M. Gambino, V. Vassiliev, J.P. Bros, J. Alloys Comp. 176 (1991) 13.
[2] G. Borzone, N. Parodi, R. Ferro, M. Gambino, J.P. Bros, J. Alloys Comp. 201 (1993) 17.
[3] A. Inoue, K. Ohtera, A.P. Tsai, T. Masumoto, Jpn. J. Appl. Phys. 27 (1988) L479.
[4] A. Inoue, K. Ohtera, A.P. Tsai, T. Masumoto, in: M. Doyama, S. Somiya, R.P.H. Chang (Eds.), Proceedings of the MRS International Meeting on Advanced Materials, Vol. 3, MRS, Pittsburgh, 1989, p. 411.
[5] K.A. Gschneidner Jr., F.W. Calderwood, Bull. Alloy Phase Diagrams 9 (1988) 686.
[6] K.H.J. Buschow, Philips Res. Rep. 20 (1965) 337.
[7] A. Saccone, A.M. Cardinale, S. Delfino, R. Ferro, Z. Metallkd. 87 (1996) 82.
[8] V.I. Kononenko, S.V. Golubev, Izv. Akad. Nauk SSSR, Met. 2 (1990) 197.
[9] T.B. Massalski et al. (Ed.), 2nd Edition, Binary Alloy Phase Diagrams, Vols. 1–3, ASM, Metals Park, OH, USA, 1990.
[10] K.A. Gschneider Jr., Physical properties of the rare earth metals, in: K.A. Gschneidner Jr., L. Eyring (Eds.), Handbook on the Physics and Chemistry of Rare Earths, Cumulative Index, Vols. 1–15, North-Holland, Elsevier, The Netherlands, 1993, p. 509.
[11] I. Barin, O. Knacke, O. Kubaschewski, Thermochemical Properties of Inorganic Substances, Springer-Verlag, Berlin, Germany, 1977.
[12] K.A. Gschneidner Jr., F.W. Calderwood, Bull. Alloy Phase Diagrams 10 (1989) 31.
[13] K.H.J. Buschow, J.H.N. van Vucht, Z. Metallkd. 57 (1966) 162.
[14] K.H.J. Buschow, J.H.N. van Vucht, Philips Res. Rep. 22 (1967) 233.
[15] A.H. Gomes de Mesquita, K.H.J. Buschow, Acta Crystallogr. 22 (1967) 497.
[16] M.E. Drits, E.S. Kadaner, N.D. Shoa, Izv. Akad. Nauk SSSR, Met. 1 (1969) 219; transl. Russ. Metall. 1 (1969) 113.
[17] L.F. Mondolfo, Aluminium Alloys: Structure and Properties, Butterworths, London, 1976, p. 355.

[18] H. Okamoto, J. Phase Equilibria 14 (1993) 395.

[19] K.H.J. Buschow, J. Less Common Metals 9 (1965) 452.

[20] K.A. Gschneidner Jr., F.W. Calderwood, Bull. Alloy Phase Diagrams 10 (1989) 28.

[21] H. Okamoto, J. Phase Equilibria 12 (1991) 395.

[22] G. Borzone, A.M. Cardinale, N. Parodi, G. Cacciamani, J. Alloys Comp. 247 (1997) 141.

[23] R. Ferro, G. Borzone, N. Parodi, G. Cacciamani, J. Phase Equilibria 15 (1994) 317.

[24] G. Borzone, A.M. Cardinale, G. Cacciamani, R. Ferro, Z. Metallkd. 84 (1993) 635.

[25] G. Canneri, A. Rossi, Gazz. Chim. Ital. 62 (1932) 202.

[26] G. Canneri, A. Rossi, Gazz. Chim. Ital. 63 (1933) 182.

[27] C. Colinet, A. Pasturel, K.H.J. Buschow, J. Chem Thermodyn. 17 (1985) 1133.

[28] F. Sommer, M. Keita, H.G. Krull, B. Predel, J.J. Lee, J. Less-Common Met. 137 (1988) 267.

[29] W.G. Jung, O.J. Kleppa, L. Topor, J. Alloys Comp. 176 (1991) 309.

[30] S.V. Meschel, O.J. Kleppa, J. Alloys Comp. 197 (1993) 75.

[31] Yu.O. Esin, S.P. Kolesnikov, V.M. Baev, M.S. Petrushevskii, P.V. Gel'd, Zh. Fiz. Khim. 55 (6) (1981) 1587.

[32] V.I. Kononenko, V.G. Shevchenko, A.L. Sukhman, Izv. Akad. Nauk SSSR, Met. 1 (1978) 67.

[33] V.I. Kober, I.F. Nichkov, S.P. Raspopin, A.G. Osval'd, Izv. Vyssh. Uchebn. Zaved., Tsvetn. Metall. 5 (1984) 125.

[34] V.G. Shevchenko, V.I. Kononenko, A.L. Sukhman, Zh. Fiz. Khim. 53 (5) (1979) 1351.

[35] G.N. Zviadadze, L.A. Chkhikvadze, M.V. Kereselidze, Soobshch. Akad. Nauk Gruz. SSR 81 (1) (1976) 149.

[36] V. Vassiliev, M. Bykov, M. Gambino, J.P. Bros, Z. Metallkd. 84 (1993) 7.